FERMILAB-PUB-06-480-A

High-energy neutrinos from astrophysical accelerators of cosmic ray nuclei

Luis A. Anchordoqui,[1] Dan Hooper,[2] Subir Sarkar,[3] and Andrew M. Taylor[4]

[1] *Department of Physics, University of Wisconsin-Milwaukee, P O Box 413, Milwaukee, WI 53201, USA*
[2] *Fermi National Accelerator Laboratory, Theoretical Astrophysics, Batavia, IL 60510, USA*
[3] *Rudolf Peierls Centre for Theoretical Physics, University of Oxford, 1 Keble Road, Oxford OX1 3NP, UK*
[4] *Astrophysics, University of Oxford, Denys Wilkinson Building, Keble Road, Oxford OX1 3RH, UK*
now at: Max-Planck-Institut für Kernphysik, Postfach 103980, D-69029 Heidelberg, GERMANY

Ongoing experimental efforts to detect cosmic sources of high energy neutrinos are guided by the expectation that astrophysical accelerators of cosmic ray protons would also generate neutrinos through interactions with ambient matter and/or photons. However there will be a reduction in the predicted neutrino flux if cosmic ray sources accelerate not only protons but also significant numbers of heavier nuclei, as is indicated by recent air shower data. We consider plausible extragalactic sources such as active galactic nuclei, gamma-ray bursts and starburst galaxies and demand consistency with the observed cosmic ray composition and energy spectrum at Earth after allowing for propagation through intergalactic radiation fields. This allows us to calculate the expected neutrino fluxes from the sources, normalized to the observed cosmic ray spectrum. We find that the likely signals are still within reach of next generation neutrino telescopes such as IceCube.

PACS numbers: 95.85.Ry, 98.70.Rz, 98.54.Cm, 98.54.Ep

I. INTRODUCTION

It has long been recognised that high energy protons produced in cosmic ray accelerators would also generate an observable flux of cosmic neutrinos, mainly through pion production in collisions with the ambient gas or with radiation fields [1]. Neutrino telescopes such as AMANDA/IceCube [2], ANTARES [3], RICE [4], ANITA [5] and the Pierre Auger Observatory [6] have presented initial results and are approaching the level of sensitivity thought to be required to detect the first high-energy cosmic neutrinos [7].

Candidate sources of high-energy neutrinos are of both Galactic and extragalactic varieties, the latter being expected to dominate at the highest energies just as for the parent cosmic rays. Likely Galactic sources include microquasars [8] and supernova remnants [9], while possible extragalactic sources include active galactic nuclei (AGN) [10], gamma-ray bursts (GRBs) [11], and starburst galaxies [12]. If however the cosmic ray sources accelerate heavy nuclei, the resulting high energy neutrino spectrum may be altered considerably from the all-proton picture which is usually assumed. Nuclei undergoing acceleration can interact with radiation fields in or near the cosmic ray engine, causing them to photo-disintegrate into their constituent nucleons which can then proceed to generate neutrinos through photo-pion interactions. Hence if most of the accelerated nuclei are broken up into nucleons before they can escape from their sources, the neutrino spectrum will not differ much from that predicted for proton accelerators. However if the radiation fields surrounding the sources are not sufficiently dense to fully disintegrate cosmic ray nuclei, fewer nucleons will be freed, leading to a reduced neutrino flux. In fact heavy nuclei can directly photo-produce pions on radiation fields but since the photo-pion production threshold is much higher than typical photo-disintegration thresholds, such interactions will be unimportant except at very high energies, well beyond the Galactic/extragalactic transition in the cosmic ray spectrum. Of course both nuclei and nucleons can scatter inelastically with ambient gas surrounding the sources to produce pions which subsequently decay into neutrinos.

In this article, we explore the impact of primary nuclei on the generation of high energy neutrinos in plausible extragalactic sources of cosmic rays. In Sec. II, we revisit the "Waxman-Bahcall bound" on the high-energy cosmic neutrino spectrum and generalize their argument to include cosmic ray nuclei. In Sec. III we estimate the photo-nuclear interaction rates for three suggested high-energy cosmic ray accelerators: AGN, GRBs, and starburst galaxies. We find that from AGN, nuclei with energies below $\sim 10^{19}$ eV can escape largely intact, while by $10^{19.5}$ eV most iron nuclei will suffer violently and only nucleons or light nuclei are expected to escape. In the case of GRB, most energetic nuclei will undergo complete disintegration and only nucleons can be emitted as cosmic rays. Starburst galaxies by contrast are ideal candidates for the emission of ultra-high energy cosmic ray nuclei, as very few nucleons are dissociated. (Recently, accretion shocks around galaxy clusters have also been invoked in this context [13].) In Sec. IV we discuss the implications of these results and derive the neutrino fluxes associated with the observed ultra-high energy cosmic rays under the assumption that their sources are optically-thin. To normalize the fluxes we require that their energy spectrum and chemical composition at Earth, after propagation through intergalactic radiation backgrounds, are consistent with experimental data from Auger and HiRes. In Sec. V we show that the expected

cosmic neutrino fluxes are still detectable by kilometer scale neutrino telescopes, such as IceCube. Our conclusions are presented in Sec. VI.

II. THE WAXMAN-BAHCALL BOUND

Waxman and Bahcall [14] pointed out some time ago that an upper bound can be placed on the diffuse flux of cosmic neutrinos assuming that they are generated in cosmologically distributed, optically-thin proton accelerators (see also Refs. [15] and [16]). In this Section, we discuss how this bound is affected if the accelerated particles are nuclei rather than protons.

First we briefly outline the original argument as applied to proton accelerators. If the observed flux of ultra-high energy cosmic rays is the result of cosmologically distributed sources, then the energy injection rate in the $10^{19} - 10^{21}$ eV) energy range can be inferred to be [17]:

$$E_{\rm CR}^2 \frac{d\dot{N}_{\rm CR}}{dE_{\rm CR}}\bigg|_{E_0} = \frac{\dot{\epsilon}_{\rm CR}^{[10^{19},10^{21}]}}{\ln(10^{21}/10^{19})} \approx 10^{44}\,{\rm erg\,Mpc^{-3}yr^{-1}}\ , \tag{1}$$

where an energy spectrum $\propto E^{-2}$ has been assumed and $E_0 = 10^{19}$ eV. The energy density of neutrinos produced through photo-pion interactions of these protons can be directly tied to the injection rate of cosmic rays:

$$E_\nu^2 \frac{dN_\nu}{dE_\nu} \approx \frac{3}{8}\epsilon_\pi\, t_{\rm H}\, E_{\rm CR}^2 \frac{d\dot{N}_{\rm CR}}{dE_{\rm CR}}, \tag{2}$$

where $t_{\rm H}$ is the Hubble time and ϵ_π is the fraction of the energy which is injected in protons lost to photo-pion interactions. (The factor of 3/8 comes from half of the pions being neutral, thus not generating neutrinos, and one quarter of the energy of charged pion decays – $\pi^+ \to \mu^+\nu_\mu \to e^+\nu_e\nu_\mu\bar{\nu}_\mu-$ going to electrons rather than neutrinos.) Thus the expected neutrino flux is:

$$\begin{aligned}[E_\nu^2\Phi_\nu]_{\rm WB} &\approx (3/8)\,\xi_Z\,\epsilon_\pi\,t_{\rm H}\,\frac{c}{4\pi}\,E_{\rm CR}^2\frac{d\dot{N}_{\rm CR}}{dE_{\rm CR}} \\ &\approx 2.3\times10^{-8}\,\epsilon_\pi\,\xi_Z\,{\rm GeV\,cm^{-2}\,s^{-1}\,sr^{-1}},\end{aligned} \tag{3}$$

where the parameter ξ_Z accounts for the effects of source evolution with redshift, and is expected to be of order unity. The "Waxman-Bahcall bound" is defined by the condition $\epsilon_\pi = 1$. For interactions with the ambient gas (i.e., pp rather than $p\gamma$ collisions), the average fraction of the total pion energy carried by charged pions is 2/3, compared to 1/2 in the photo-pion channel. In this case, the upper bound given in Eq. (3) is enhanced by 33% [18].

At production, the neutrino flux consists of equal fractions of ν_e, ν_μ and $\bar{\nu}_\mu$. Originally, the Waxman-Bahcall bound was presented for the sum of ν_μ and $\bar{\nu}_\mu$ (neglecting ν_e), motivated by the fact that only muon neutrinos are detectable as track events in neutrino telescopes. Since oscillations in the neutrino sector mix the different species, we chose instead to discuss the sum of all neutrino flavors. When the effects of oscillations are accounted for, nearly equal numbers of the three neutrino flavors are expected at Earth. Note that IceCube will be capable of detecting and discriminating between all three flavors of neutrinos [19].

Electron antineutrinos can also be produced through neutron β-decay. This contribution, however, turns out to be negligible. To obtain an estimate, we sum over the neutron-emitting sources out to the edge of the universe at a distance $\sim 1/H_0$ [20]:

$$\Phi_{\overline{\nu}_e} = \frac{m_n\,\xi_Z}{8\,\pi\,\epsilon_0\,H_0}\int_{\frac{m_n E_{\overline{\nu}}}{2\epsilon_0}}^{E_n^{\rm max}} \frac{dE_n}{E_n}\,\frac{d\dot{N}_n}{dE_n}\ , \tag{4}$$

where $d\dot{N}_n/dE_n$ is the neutron volume emissivity and m_n the neutron mass. Here, we have assumed that the neutrino is produced monoenergetically in the neutron rest frame, i.e., $\epsilon_0 \sim \delta m(1 - m_e^2/\delta_m^2)/2 \sim 0.55$ MeV, where $\delta m \simeq 1.30$ MeV is the neutron-proton mass difference. An upper limit can be placed on $d\dot{N}_n/dE_n$ by assuming an extreme situation in which all the cosmic rays escaping the source are neutrons, i.e.,

$$\dot{\epsilon}_{\rm CR} = \int dE_n\ E_n\ \frac{d\dot{N}_n}{dE_n}\,. \tag{5}$$

With the production rate of ultra-high energy protons $\dot{\epsilon}_{\rm CR}^{[10^{19},10^{21}]} \sim 5\times10^{44}$ erg Mpc^{-3} yr^{-1} [17], and an assumed injection spectrum $d\dot{N}_n/dE_n \propto E_n^{-2}$, Eq. (4) gives

$$E_\nu^2\Phi_{\overline{\nu}_e} \approx 3\times10^{-11}\,\xi_Z\ {\rm GeV\,cm^{-2}\,s^{-1}\,sr^{-1}}\ , \tag{6}$$

which is about three orders of magnitude below the Waxman-Bahcall bound in Eq.(3).

If the injected cosmic rays include nuclei heavier than protons, then the neutrino flux expected from the cosmic ray sources may be modified. Nuclei undergoing acceleration can produce pions, just as protons do, through interactions with the ambient gas, so the Waxman-Bahcall argument would be unchanged in this case. However if interactions with radiation fields dominate over interactions with matter, the neutrino flux would be suppressed if the cosmic rays are heavy nuclei. This is because the photo-disintegration of nuclei dominates over pion production at all but the very highest energies. Defining κ as the fraction of nuclei heavier than protons in the observed cosmic ray spectrum, the resulting neutrino flux is then given by:

$$E_\nu^2\Phi_\nu \approx (1-\kappa)\ [E_\nu^2\Phi_\nu]_{\rm WB}\ . \tag{7}$$

The Waxman-Bahcall bound can be turned into a flux prediction by making further assumptions. For example one can assume that all charged particles remain trapped within the acceleration region and only neutrons are able to escape. If this were the case, the energy fraction of cosmic ray protons lost to photo-pion interactions can be easily obtained from single pp or $p\gamma$ collisions, yielding $\epsilon_\pi \sim 0.2 - 0.6$. This flux estimate, however, does

not account for production of protons at the source edge (which would have a large probability of escaping the acceleration region), threshold effects (near the photo-pion production threshold, the assumed relationship between the average energy of the incoming proton and that of the outgoing neutrino can be signifcantly altered), and energy degradation of the charged pions propagating through the (possibly strong) magnetic fields in the plasma. In the remainder of this paper, we will estimate the flux of cosmic neutrinos from specific astrophysical sites, taking into account all of these considerations and assuming that high energy cosmic rays are constituted of both protons and nuclei, in conformity with observational data on their spectrum and composition.

III. PHOTO-REACTION RATES FOR PROTONS AND NUCLEI: THREE CASE EXAMPLES

It is likely that the bulk of the cosmic radiation is created as a result of some general magneto-hydrodynamic process which channels kinetic or magnetic energy of cosmic plasmas into charged particles. The details of the acceleration process and the maximum attainable energy depend on the time scale over which particles are able to interact with the plasma. Sometimes the acceleration region itself only exists for a limited period of time (e.g. supernovae shock waves dissipate after about 10^4 yr). If the plasma disturbances persist for long periods, the maximum energy may be limited by the likelihood of escape from the region. If one includes the effect of the characteristic velocity, βc, of the magnetic scattering centres, the above argument leads to the so-called "Hillas criterion" for the maximum energy acquired by a charged particle moving in a medium with magnetic field B, $E_{\rm max} \sim 2\beta\, c\, Ze\, B\, r_{\rm L}$, where $r_{\rm L} \approx Z^{-1}(B/\mu{\rm G})^{-1}$ kpc is the Larmor radius of cosmic rays with charge Ze [21]. In what follows, we consider the radiation fields associated with three classes of potential cosmic ray sources and determine the particle's energy loss rate, assuming that within these sources the trapping condition for efficient acceleration is fulfilled up to the highest energies [22].

There are basically four ways in which ultra-high energy cosmic rays interact with ambient photons: Compton interactions, photo-pair production in the field of the nucleon/nucleus, photo-disintegration of the nucleus, and photo-production of hadrons (mainly pions). Although Compton scattering has no energy threshold, it results in a negligibly small energy loss rate for high energy cosmic rays, so we will not consider it further. Photo-pair and photo-pion production occur at center-of-mass energies higher than $E^{e^+e^-}_{\rm th} = 2m_e \simeq 1$ MeV and $E^{\pi}_{\rm th} = m_\pi(1 + m_\pi/2m_p) \simeq 145$ MeV, respectively. The relative contributions of these two processes to the total energy losse is dictated by the ratio of the product of the corresponding inelasticity and cross-section. For a relativistic nucleon, this product has an average value of $\sim 5 \times 10^{-31}{\rm cm}^2$ from threshold up to ~ 500 MeV in the case of photo-pair production, and an average value of $\sim 7 \times 10^{-29}{\rm cm}^2$ from threshold up to ~ 200 GeV for the case of photo-pion production [23]. For nuclei, the energy loss rate due to photo-pair production is Z^2/A times higher than for a proton of the same Lorentz factor [24], whereas the energy loss rate due to photo-meson production remains roughly the same (because the cross-section for photo-meson production by nuclei is proportional to the mass number A [25], while the inelasticity is proportional to $1/A$). However, it is photo-disintegration rather than photo-pair and photo-meson production that determines the energetics of ultra-high energy cosmic ray nuclei [26]. Experimental data on photo-nuclear interactions are consistent with a two-step process: photo-absorption by the nucleus to form a compound state, followed by a statistical decay process involving the emission of one or more nucleons. Details of how the relevant cross sections for all these processes are calculated and the energy loss rates implemented in our simulation can be found in Ref. [27].

A. Active Galactic Nuclei

Among known non-thermal sources in the universe, radio–loud AGN seem to be the most energetic [28] hence they have long been suspected to be likely accelerators of ultra-high energy cosmic rays [29]. At radio frequencies where very large baseline interferometers can resolve the emission regions on milliarcsecond scales, many radio–loud AGN exhibit highly collimated jets of relativistic plasma with opening angles of a few degrees or less. AGN come in various guises according to the orientation of their radio jets and the characteristics of the circum-nuclear matter in their host galaxies. The most extreme versions are Fanaroff Riley radio-galaxies whose radio jet axes are almost in the plane of the sky, and blazars which have the radio jet axes aligned close to the line-of-sight to the observer (yielding a significant flux enhancement through Doppler boosting).

A total of 66 blazars have been detected to date as GeV γ-ray sources by EGRET [30]. In addition, observations from ground-based air Čerenkov telescopes indicate that in at least two of these sources the γ-ray spectrum extends above a TeV [31]. The non-thermal emission of these powerful objects shows a triple-peak structure in the overall spectral energy distribution. The first component (from radio to X-rays) is generally interpreted as being due to synchrotron radiation from a population of non-thermal electrons, the second (UV) component as blackbody radiation originating from the accretion disk, and the third component (γ-rays) is explained either as due to inverse Compton scattering of the same electron population on the various photon fields traversed by the jet [32], or by the decay of neutral pions produced when the highly relativistic baryonic outflow collides with diffuse gas targets moving across the jet [33].

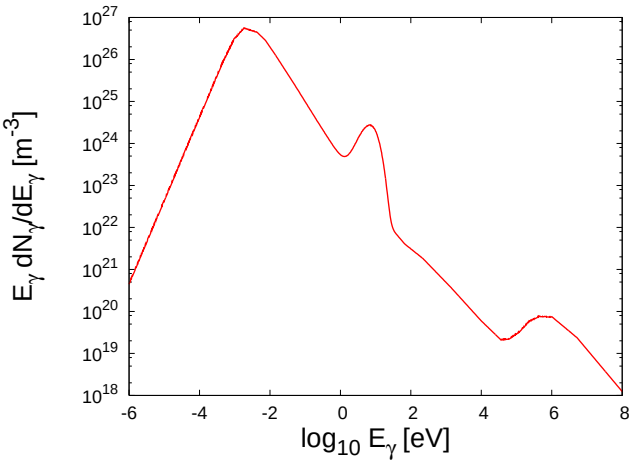

FIG. 1: The photon energy spectrum of a flaring blazar as seen in the observer's frame. The normalization is obtained from the condition $U_\gamma/E_\gamma^{\rm peak} = E_\gamma^{\rm peak} {\rm d}N/{\rm d}E_\gamma\big|_{\rm peak}$.

For the background radiation spectrum in AGN, we adopt the Böttcher blazar flaring state model [34]. The two relevant components are synchotron radiation peaking at $E_\gamma^{\rm peak} \sim 0.003$ eV, then falling as $dN_\gamma/dE_\gamma \propto E_\gamma^{-2.3}$, and a 20,000 K blackbody radiation from the accretion disk. It is assumed that 10% of the Eddington luminosity is radiated as blackbody radiation and 1% as synchrotron radiation [35].

The cosmic ray acceleration process is assumed to occur within a relativistic blob of plasma moving along the jet with Lorentz factor $\Gamma \sim 10^{1.5}$. In the rest frame of the plasma, the blob is assumed to be spherical with radius $R' = c\Delta t' = \Gamma c \Delta t$, where $\Delta t \approx 10^4$ s indicates the typical duration of a flare. The energy density injected into such a blob can be estimated from the apparent bolometric luminosity, L_γ, and the duration of flare

$$U_\gamma = \frac{L_\gamma\, \Delta t}{(4\pi/3)\, (c\,\Delta t)^3} \approx 6\times 10^{24} \left(\frac{L}{10^{45}\ {\rm erg/s}}\right) \left(\frac{\Delta t}{10^4\ {\rm s}}\right)^2\ {\rm eV\,m^{-3}}. \quad (8)$$

The spectrum of background photons is shown in Fig. 1. Note that since the blob is relativistic, $L'_\gamma \Delta t' = L_\gamma \Delta t/\Gamma$, implying a significant dilution of the energy density in the plasma rest frame,

$$U'_\gamma = \frac{L'_\gamma \Delta t'}{(4/3)\,(c\Delta t')^3} = \frac{U_\gamma}{\Gamma^4}\,. \quad (9)$$

The fraction of the total energy in cosmic ray protons, E'_p, expected to be lost within the acceleration region to pion production is just,

$$\epsilon_\pi(E'_p) \approx \frac{R'}{l_\pi(E'_p)}\ , \quad (10)$$

where

$$l_\pi(E'_p) = \frac{E_\gamma'^{\rm peak}}{K_p(E'_p) U'_\gamma \sigma_\Delta} = \frac{\Gamma^4\, E_\gamma'^{\rm peak}}{K_p(E'_p)\ U_\gamma\ \sigma_\Delta} \quad (11)$$

is the proton attenuation length due to interactions with the radiation field, σ_Δ is the cross-section, and $K(E'_p)$ is the inelasticity of a single collision. (Recall that primed quantities refer to the plasma rest frame). For protons interacting via the Δ-resonance we find,

$$\epsilon_\pi \approx \left(\frac{3\times 0.2}{4\pi\Gamma^2}\right)\left(\frac{L_\gamma \Delta t}{E_\gamma^{\rm peak}}\right)\left[\frac{\sigma_\Delta}{(c\Delta t)^2}\right] \approx 553 \left(\frac{10^{1.5}}{\Gamma}\right)^2 \left(\frac{L_\gamma}{10^{45}\ {\rm erg/s}}\right)\left(\frac{3\times 10^{-3}\ {\rm eV}}{E_\gamma^{\rm peak}}\right)\left(\frac{10^4\ {\rm s}}{\Delta t}\right)\ ,$$

where the inelasticity, $K_p(E'_p) \approx 0.2$, is kinematically determined by requiring equal boosts for the decay products of the Δ [36]. A straightforward calculation shows that the required proton energy for Δ-resonant production at the peak of the photon distribution is,

$$E'_p = \frac{(m_\Delta c^2)^2 - (m_p c^2)^2}{4E_\gamma'^{\rm peak}} \approx 10^{21.2}\ {\rm eV}, \quad (12)$$

where $m_\Delta \simeq 1232$ MeV is the mass of the resonance and m_p the proton mass. In Fig. 2 we show the expected photo-pion production and photo-disintegration rates for protons and nuclei. It is clear that the radiation field becomes thick to photo-pion interactions at an energy (in the observer's frame) of $E_p \approx 10^{18}$ eV (which corresponds to $E'_p \approx 10^{19.5}$ eV), whereas it becomes opaque to the propagation of nuclei about a decade lower in energy. One can also verify that photo-disintegration dominates over photo-pion production by nuclei at all energies, hence neutrino production through photo-nuclear interactions can be safely neglected.

B. Gamma Ray Bursts

GRBs are flashes of high energy radiation that can be brighter, during their brief existence, than any other source in the sky. The bursts present an amazing variety of temporal profiles, spectra, and timescales [37].

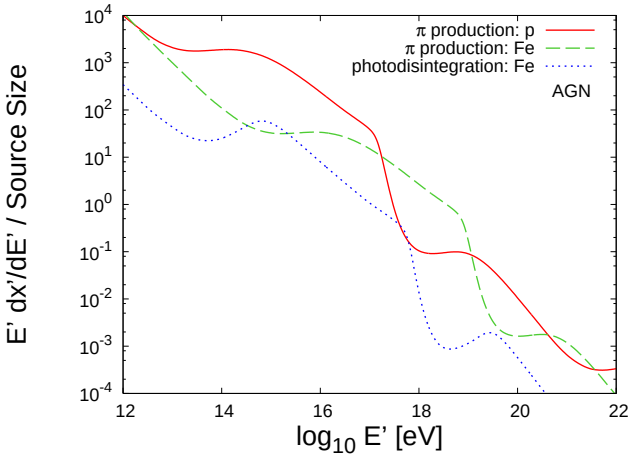

FIG. 2: Comparison of the rates for photo-pion production by protons, photo-pion production by iron nuclei and photo-disintegration of iron nuclei, as a function of the proton/iron nucleus energy in the rest frame of the AGN plasma. The source size is normalized such that $E'\mathrm{d}x'/\mathrm{d}E' = K_p(E'_p)/\epsilon_\pi$ at the peak energy, which corresponds to a proton energy $E' \equiv E'_p \simeq 10^{21.2}$ eV. The photo-disintegration and photo-pion production rates for iron nuclei are normalized using the number density of photons given in Fig. 1.

Our insights into this phenomenon have been increased dramatically by BATSE observations of over 2000 GRBs, and more recently, by data from SWIFT [38].

There are several classes of bursts, from single-peaked events, including the fast rise and exponential decaying (FREDs) and their inverse (anti-FREDs), to chaotic structures [39]. There are well separated episodes of emission, as well as bursts with extremely complex profiles. Most of the bursts are time asymmetric but some are symmetric. Burst timescales range from about 30 ms to several minutes.

The GRB angular distribution appears to be isotropic, suggesting a cosmological origin [40]. Furthermore, the detection of "afterglows" — delayed low energy (radio to X-ray) emission — from GRBs has confirmed this via the redshift determination of several GRB host-galaxies [41].

If the sources are so distant, the energy necessary to produce the observed events by an intrinsic mechanism is astonishing: about 10^{51} erg of gamma rays must be released in less than 1 second. The most popular interpretation of the GRB-phenomenology is that the observable effects are due to the dissipation of the kinetic energy of a relativistic expanding plasma wind, a "fireball" [42]. Although the primal cause of these events is not fully understood, it is generally believed to be associated with the core collapse of massive stars (in the case of long duration GRBs) and stellar collapse induced through accretion or a merger (short duration GRBs) [43].

The very short timescale observed in the time profiles indicate an extreme compactness that implies a source which is initially opaque (because of $\gamma\gamma$ pair creation) to γ-rays. The radiation pressure on the optically thick source drives relativistic expansion, converting internal energy into the kinetic energy of the inflating shell. Baryonic pollution in this expanding flow can trap the radiation until most of the initial energy has gone into bulk motion with Lorentz factors of $\Gamma \sim 10^2 - 10^3$ [44]. (In our calculations we set $\Gamma = 10^{2.5}$). The kinetic energy can be partially converted into heat when the shell collides with the interstellar medium or when shocks within the expanding source collide with one another. The randomized energy can then be radiated by synchrotron radiation and inverse Compton scattering yielding non-thermal bursts with timescales of seconds. Charged particles may be efficiently accelerated to ultra-high energies in the fireball's internal shocks, hence GRBs are often considered as potential sources of cosmic rays [45].

To describe the radiation fields associated with GRBs, we adopt a standard broken power-law spectrum: $\mathrm{d}N_\gamma/\mathrm{d}E_\gamma \propto E_\gamma^{-\beta}$, where $\beta = 1, 2$ respectively at energies below and above the break energy, $E_\gamma^{\rm break} = 1$ MeV [11], which fits the BATSE data well [46]. In many ways the situation is similar to the blob of emitted plasma in the AGN model. However, in the fireball's *comoving* frame, a spherical shock expands relativistically in all directions (with Lorentz factor Γ), and thus a change in geometry is required. In a frame moving with Lorentz factor Γ towards the observer, the shock has thickness R/Γ, where R is the initial size of the compact object before the fireball phase. In the observer's frame, the shock is further compressed into a thin shell of thickness R/Γ^2. Therefore, the fiducial value for the energy density, U'_γ, of a shell of luminosity, L'_γ, radius R', and thickness R'/Γ is [47],

$$U'_\gamma = \frac{\Gamma\ L'_\gamma\ \Delta t'}{4\pi\ R'^3} = \frac{L_\gamma \Delta t}{\Gamma^6 4\pi (c\Delta t)^3} = 1\times 10^{27} \left(\frac{10^{2.5}}{\Gamma}\right)^6 \left(\frac{L_\gamma}{10^{51}\ \mathrm{erg\ s^{-1}}}\right) \left(\frac{5\times 10^{-2}\ \mathrm{s}}{\Delta t}\right)^2\ \mathrm{eV\ m^{-3}} \tag{13}$$

where $R' = \Gamma^2\, c\Delta t$. The spectrum of this radiation field is shown in Fig. 3.

The fraction of energy deposited in the GRB by an ultra-relativistic proton of energy E'_p is,

$$\epsilon_\pi(E'_p) \approx \left(\frac{K_p(E'_p)}{4\pi\Gamma^5}\right) \left(\frac{L_\gamma \Delta t}{E'^{\rm break}_\gamma}\right) \left(\frac{\sigma_\Delta}{(c\Delta t)^2}\right)\ . \tag{14}$$

For protons interacting through the Δ-resonance with photons of energy $E_\gamma'^{\rm break} \simeq 10$keV, Eq. (14) yields:

$$\epsilon_\pi \approx \left(\frac{0.2}{4\pi\Gamma^4}\right)\left(\frac{L_\gamma \Delta t}{E_\gamma^{\rm break}}\right)\left(\frac{\sigma_\Delta}{(c\Delta t)^2}\right) = 0.2\left(\frac{10^{2.5}}{\Gamma}\right)^4\left(\frac{L_\gamma}{10^{51}\ {\rm erg\ s^{-1}}}\right)\left(\frac{1\ {\rm MeV}}{E_\gamma^{\rm break}}\right)\left(\frac{5\times10^{-2}\ {\rm s}}{\Delta t}\right)\ . \quad (15)$$

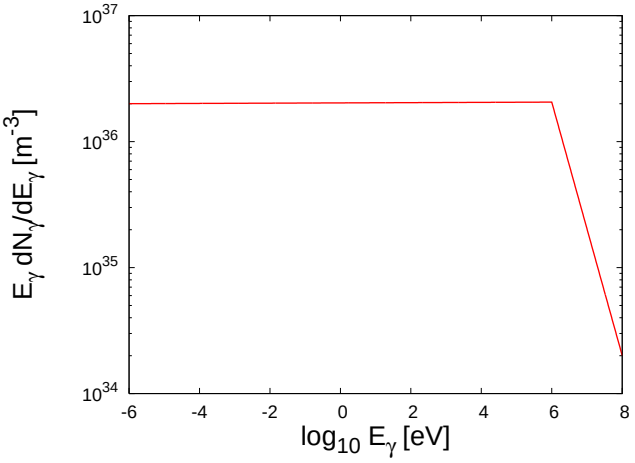

FIG. 3: The photon energy spectrum of a GRB as seen in the observer's frame. The normalization is obtained from the condition $U_\gamma/E_\gamma^{\rm break} = E_\gamma^{\rm break}{\rm d}N/{\rm d}E_\gamma\big|_{\rm break}$.

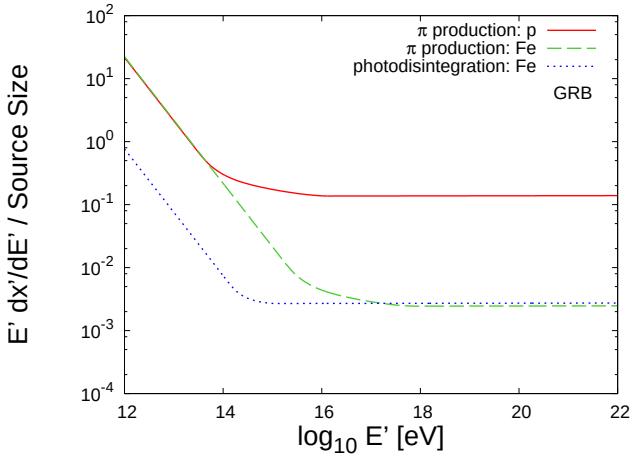

FIG. 4: Comparison of the photo-pion production and photo-disintegration interaction rates as a function of the proton/iron nucleus energy in the rest frame of a GRB fireball. The source size is normalized such that 20% of the accelerated protons at a laboratory (observer's) energy of 10^{16} eV are converted to pions.

In Fig. 4 we show the expected photo-pion production and photo-disintegration rates for protons and nuclei. This figure highlights that (with our assumptions) GRBs are expected to be optically thin to $p\gamma$ interactions, with protons undergoing at most one interaction before leaving the source region. It is worthwhile pointing out that although the nucleus photo-disintegration and photo-pion production rates become comparable at laboratory (observer) energies $E > 10^{16}$ eV, most of the charged pions produced in this energy regime readily lose energy through synchroton radiation in the strong $\vec{B}$-field of the fireball. For example, at 10^{17} eV only 1% of the produced pions decay before losing a significant fraction of their energy. Since the neutrino flux falls by more than two orders of magnitude per decade increase in energy, the contribution from pions suffering energy degradation would be negligible, and therefore can be ignored.

C. Starbursts

Starbursts, galaxies undergoing an episode of large-scale star formation, have also been proposed as sources of ultra-high energy cosmic rays [48]. These environments feature strong infrared emission by dust associated with high levels of interstellar extinction, strong UV spectra from the Lyman α emission of hot OB stars, and considerable radio emission produced by recent supernova remnants. The central regions of starburst galaxies can be orders of magnitude brighter than those of normal spiral galaxies. From such an active region, a galactic-scale superwind (driven by the collective effect of supernovae and winds from massive stars) can conceivably accelerate cosmic ray nuclei to ultra-high energies.

The Lyman-α background is powered by the rich OB and red supergiant stellar populations within the inner core of these galaxies, which typically has a radius $R \sim 100$ pc. The average density in the region depends on the temperatures $T_{\rm OB}$ and $T_{\rm SG}$ of O, B, and red supergiant stars, respectively, and the dilution due to the inverse square law. Specifically, for a region with $N_{\rm OB}$ OB stars and $N_{\rm SG}$ red supergiant stars, the photon density was estimated to be [49]

$$n = \frac{9}{4}\left[\frac{n^{\rm BE}_{T_{\rm OB}}(\epsilon)\, N_{\rm OB}\, R^2_{\rm OB} + n^{\rm BE}_{T_{\rm SG}}(\epsilon)\, N_{\rm SG}\, R^2_{\rm SG}}{R^2}\right], \quad (16)$$

where

$$n^{\rm BE}_T(\epsilon) = (\epsilon/\pi)^2\ \left[e^{\epsilon/T} - 1\right]^{-1} \quad (17)$$

is a Bose-Einstein distribution with energy ϵ and temperature T (normalized so that the total number of photons in a box is $\int n(\epsilon)d\epsilon$). Here, $R_{\rm OB(SG)}$ is the radius of the OB (SG) stars and the factor 9/4 comes from averaging the inverse squares of the distance of an observer to uniformly distributed sources in a spherical region of radius

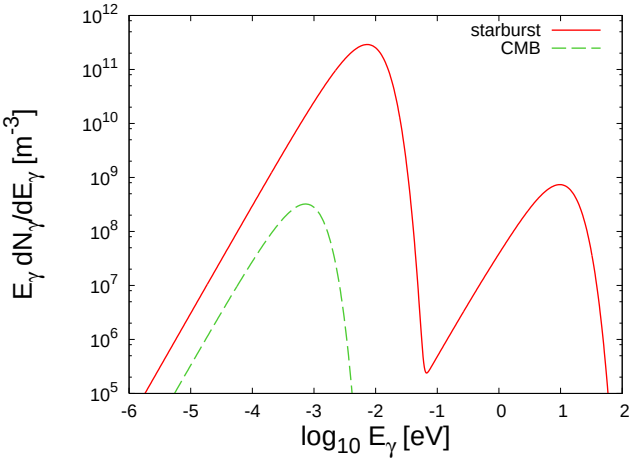

FIG. 5: Thermal photon spectrum of starburst galaxies as derived from Eq. (16). We have taken for the OB stars a surface temperature $T_{\rm OB} = 40,000$ K and radius $R_{0\rm B} = 15 R_\odot$, and for the cooler red supergiants, $T_{\rm SG} = 4,000$ K and $R_{\rm SG} = 50\odot$. The spectrum of the cosmic microwave background is shown for comparison.

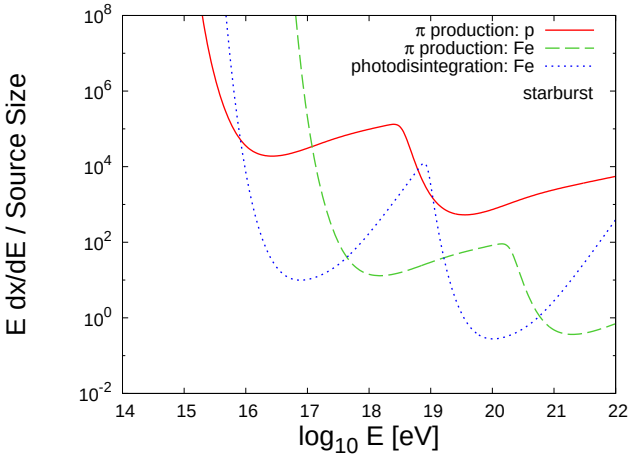

FIG. 6: Comparison of the photo-pion and photo-disintegration interaction rates as a function of the proton/iron nucleus energy in a starburst galaxy.

R [50]. We assume the OB and red supergiant stars to constitute 90% and 10%, respectively, of the total population of 27,000 [51].

We also adopt a single component dust model in which clumpy dust surrounds the starburst region, in thermal equilibrium with it and heated to a temperature of 30 K [52]. About 90% of the stellar light is assumed to be reprocessed into IR radiation and the resulting thermal photon spectrum is shown in Fig. 5.

Iron nuclei with Lorentz factors up to $\sim 10^6$ may be accelerated in supernova explosions [53]. Despite the starburst region being only about ~ 100 pc in size, most of these nuclei may be trapped there through diffusion in milli-Gauss magnetic fields [54] for $\sim 10^4$ yr [55]. However since magnetic rigidity increases with Lorentz factor, the diffusion time would decrease with rising energy. In our analysis we adopt the cosmic ray time delay

$$\tau_{\rm delay} = 400\, Z \left(\frac{E}{5 \times 10^{15}\ {\rm eV}} \right)^{-1/3} \ {\rm yr}\ , \qquad (18)$$

as expected due to trapping in a Kolmogorov spectrum of magnetic field fluctuations [56].

Combining the above estimates of the propagation time, the size of the starburst region and the number density of UV and IR photons, we find the proton and nucleus photo-production rates shown in Fig. 6. It is seen that the medium is (almost) transparent to the propagation of cosmic rays. Photo-pion production by nuclei will not be important until very high energies (Lorentz factors $\gg 10^{10}$), hence can be neglected.

Before proceeding further, it is important to note that pions produced through hadronic interaction with the ambient gas would also contribute to the flux of neutrinos. The exact intensity of this "*pp* hadronic compo-

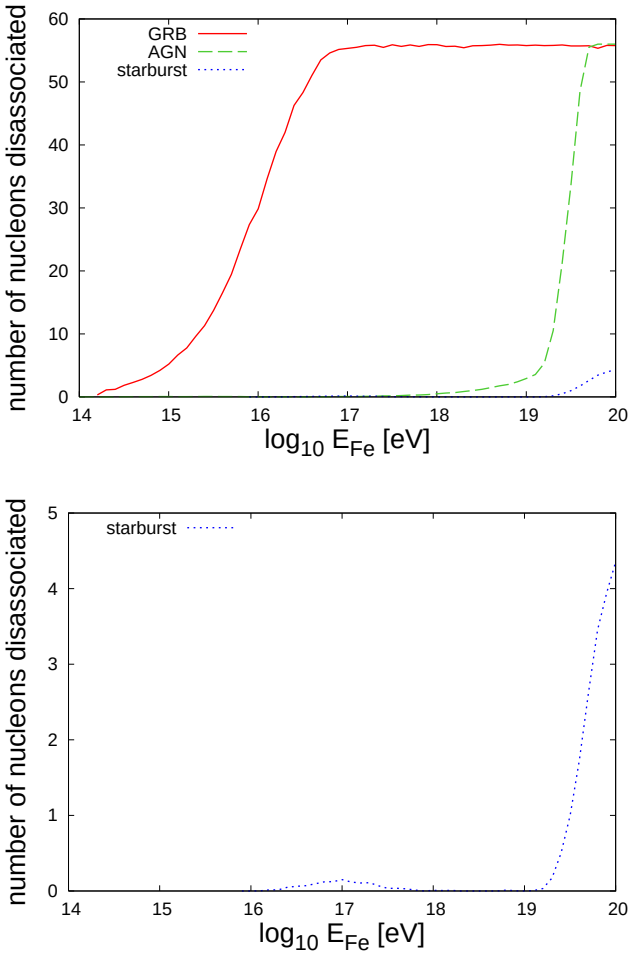

FIG. 7: The top panel shows the average number of nucleons photo-dossiciated from an iron nucleus of a given energy for the radiation field spectra of AGN, GRBs, and starbursts. The lower panel shows the starburst case in more detail.

nent" is currently under debate [12, 57] but an upper bound can certainly be placed from the non-observation of γ-rays from nearby starburst galaxies [58]. In this regard, the improved sensitivity of GLAST over EGRET is significant — detection of even a single starburst galaxy by GLAST would imply that such objects make a considerable contribution to the diffuse flux of extra-galactic neutrinos [59]. To be conservative in our calculations we do not consider contributions from the *pp* channel.

Our essential results so far can be summarized as follows with reference to Fig. 7):
(1) In AGN, nuclei with energies below about 10^{19} *eV can escape largely intact, while more energetic nuclei undergo an increasing degree of disintegration; by* $10^{19.5}$ *eV, most iron nuclei from AGN will suffer violently, and only nucleons or very light nuclei are expected to escape.*
(2) In GRB, most nuclei will undergo complete disintegration and only nucleons can be emitted as cosmic rays.
(3) Starburst galaxies are ideal candidates for the emission of ultra-high energy cosmic ray nuclei, as very few nucleons are disassociated even at the highest energies.

We can now calculate the neutrino flux associated with the observed ultra-high energy cosmic rays, taking into account observational data on their energy spectrum and showering characteristics which suggest that they consist of a *mixture of protons and heavy nuclei*, rather than being purely protons. In other respects we make the same assumptions as Waxman and Bahcall [14], e.g. that the extragalactic sources are optically thin.

IV. THE COSMIC NEUTRINO FLUX FROM EXTRAGALCTIC SOURCES

As we have seen above, cosmic ray nuclei which escape from the acceleration region unscathed do not contribute to the source neutrino spectrum. Therefore, in order to estimate the latter, we first need to determine the fraction of heavy nuclei in the high energy cosmic rays arriving at Earth, which we denote by κ.

This issue is closely connected with that of the "cross-over" energy at which a transition occurs between Galactic and extragalactic cosmic rays. It would be natural to expect a flattening of the energy spectrum at this point as the harder subdominant extragalactic component takes over from the softer Galactic component. Such an "ankle" was indeed observed by Fly's Eye [60] at $\sim 10^{18.5-18.7}$ eV which is roughly the energy at which the (proton) Larmor radius begins to exceed the thickness of the Milky Way disk and one expects the Galactic component of the spectrum to die out. The end-point of the Galactic flux ought to be dominated by heavy nuclei, as these have a smaller Larmor radius for a given energy, and the data is indeed consistent with a transition from heavy nuclei to a lighter composition at the ankle.

However recent HiRes data indicate that this change in the cosmic ray composition occurs at a much lower energy of $\sim 10^{17.6}$ eV [61], where the spectral slope steepens from E^{-3} to $E^{-3.3}$ [62]. This "second knee" in the spectrum, recognised originally in AGASA data [63], can be explained [64] as arising from energy losses of extragalactic protons over cosmic distances due to e^+e^- pair-production on the cosmic microwave background (CMB). The "ankle" is now interpreted as the minimum in the e^+e^- energy-loss feature [65] and this requires that there be an almost total absence of iron nuclei ($\lesssim 0.05\%$ for $E > 10^{18}$ eV) in extragalactic cosmic rays [66].

However the data on the composition inferred from different analyses of the characteristics of cosmic ray air showers do not support such a simple picture [67]. For example the depth of shower maximum $X_{\rm max}$ at $E > 10^{18}$ eV is *not* consistent with a pure proton composition, even allowing for the uncertainties in modelling hadronic interactions at such high enegies. This is seen in Fig. 8 where we show the evolution of $X_{\rm max}$ for both proton and iron showers as obtained from extensive air shower simulations using the program CORSIKA (version 6.20) [73] along with experimental data from Fly's Eye, HiRes and Yakutsk. The predictions of three different hadronic interaction models (DPMJET [74], SIBYLL [75], and QGSJET II [76]) are shown so that an impression of the modelling uncertainties may be gained from the spread between them.

In fact, recent analyses [27, 68] show that the $X_{\rm max}$ data, as well as the data on the energy spectrum from both HiRes [69] and the Pierre Auger Observatory [70], can *simultaneously* be reproduced if the extra-galactic cosmic rays contain a substantial fraction of heavy nuclei, and the Galactic/extra-galactic transition occurs, as was believed originally, at the "ankle" in the spectrum.

In previous work [27] we undertook a detailed calculation of the intergalactic propagation of ultra-high energy heavy nuclei through known cosmic radiation fields, in order to find the energy spectrum and composition at Earth. To keep things simple we now consider only protons and iron nuclei. Armed with our previous results, we estimate the fraction of iron nuclei, κ, in extragalactic cosmic rays, by finding the linear combination of pure iron and pure proton energy spectra that matches the Auger data [70] best, after propagation effects are accounted for. Our results, shown in Fig. 9, indicate that a mixed composition with 75% protons and 25% iron nuclei best reproduces the data (although the fit quality is poor, suggesting correlated and/or overestimated uncertainties). As seen in Fig. 8, this particular mixed composition at source also allows a good match to the $X_{\rm max}$ data. A better fit can perhaps be obtained by considering a more complex composition (e.g. reflecting the composition of matter in plausible sources) but the quality of present data is not good enough to warrant this. Even in this simple 2-component model, we obtain a distinct improvement in the fit by increasing κ from 10% to 25%, and this is consistent with the energy spectrum.

By performing a Monte Carlo simulation for cosmic ray protons and nuclei propagating through the sources con-

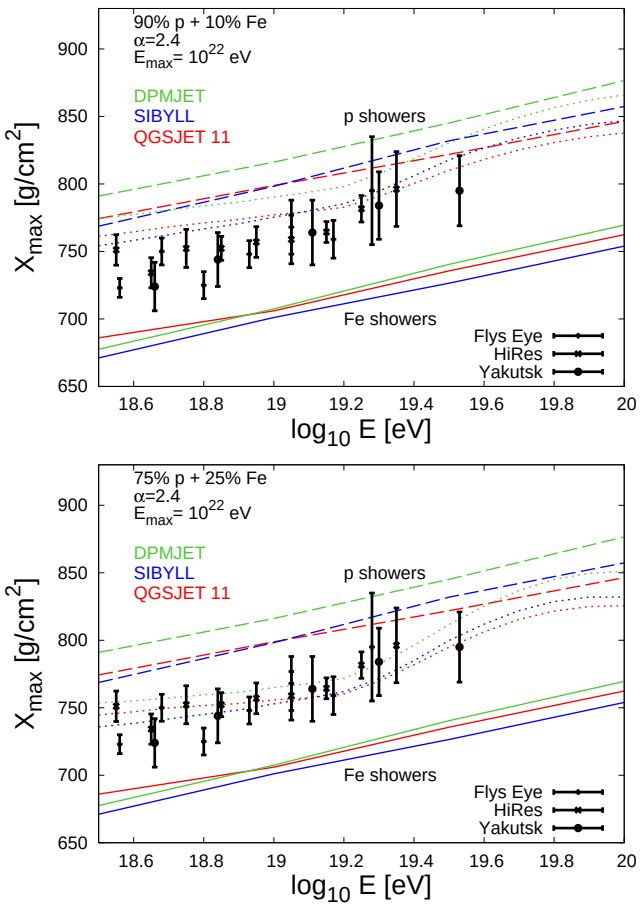

FIG. 8: The top (bottom) panel shows the depth of shower maximum, $X_{\rm max}$, for cosmic rays with energy spectrum $\propto E^{-\alpha}$ which are a mixture of 90% (75%) protons and 10% (25%) iron. The solid, dashed, and dotted lines are the predicted values of $X_{\rm max}$ for a pure iron, pure proton, and the mixed composition, respectively. The spread in the predictions for different hadronic interaction models is also shown. The experimental data are from the Fly's Eye [60], HiRes [71] and Yakutsk [72] experiments.

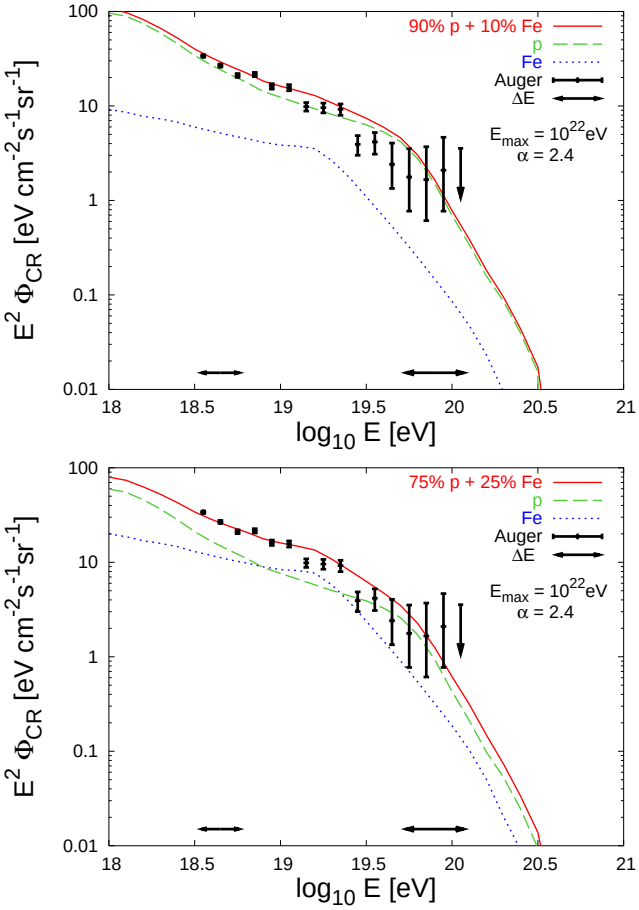

FIG. 9: Best fit of the Auger energy spectrum [70], assuming a constant comoving density of sources which emit both protons and iron nuclei with energy spectrum $\propto E^{-\alpha}$. In the fitting procedure we used data above $E_- = 10^{18.5}$ eV (top panel) and above $E_- = 10^{18.7}$ eV (lower panel), finding χ^2/d.o.f. = 52.5/15 and χ^2/d.o.f. = 41.6/13, respectively. The favoured mixture is 10% (25%) iron and 90% (75%) for $E_- = 10^{18.5}$ eV ($E_- = 10^{18.7}$ eV) — the dependence on E_- arises because lower energy points have smaller statistical uncertainties. The horizontal error bars indicate the systematic uncertainties in energy measurement.

sidered, the neutrino flux produced in each of the three case examples can now be calculated. The results shown in Fig. 10 are obtained assuming a cosmological distribution of sources which accelerate cosmic rays with a spectrum $\propto E^{-2.4}$. Using the emissivity of AGN, the corresponding peak neutrino flux is,

$$\Phi_\nu(E_\nu) \;=\; 2.3\times10^{-5}\left(1-e^{-\epsilon_\pi/K_p}\right) \times\; E_\nu^{-2.4}\,{\rm GeV}^{-1}\,{\rm cm}^{-2}\,{\rm s}^{-1}\,{\rm sr}^{-1}\;, \qquad (19)$$

where E_ν is in GeV and we have normalized to a cosmic ray production rate of:

$$\dot\epsilon_{\rm CR}^{[10^{18.7},\,10^{22.0}]} = 2.2\times10^{44}\,{\rm erg\,Mpc^{-3}yr^{-1}}\;, \qquad (20)$$

as indicated by Auger data. In the case of GRBs, because of the strong magnetic fields in the plasma, the neutrinos are created by parent protons with energies below 10^{18} eV. Following Ref. [64], we assume in this case a break in the proton injection spectrum ($\propto E^{-2}$ below 10^{18} eV), so that the corresponding peak neutrino flux saturates the Waxman-Bahcall bound, yielding

$$\Phi_\nu(E_\nu) \;=\; 1.0\times10^{-8}\left(1-e^{-\epsilon_\pi/K_p}\right) \times\; E_\nu^{-2}\,{\rm GeV}^{-1}\,{\rm cm}^{-2}\,{\rm s}^{-1}\,{\rm sr}^{-1}\;. \qquad (21)$$

Note that this normalization differs from that in Eq. (3) because of the different energy range of the source injection spectrum required to accomodate the Auger data [77].

We do not show the neutrino flux expected from starburst galaxies because it is negligible compared to than from AGN or GRBs. The interaction length of protons in

starburst galaxies is ~ 500 times the source size or larger at all energies (see Fig. 6), leading to $\epsilon_\pi \lesssim 10^{-3}$, while AGN and GRBs have $\epsilon_\pi \sim 1$. Thus the uncertainties in the modelling of starburst galaxies are immmaterial in this context.

The required bi-modal composition at source (75% protons plus 25% of heavy nuclei) does however require that sources such as starburst galaxies accelerate most of the iron nuclei, with most of the protons coming from AGN and GRBs. In Fig. 11, we show the sum of the neutrino fluxes produced by AGN and GRBs assuming they contribute approximately equally. Not surprisingly, the predicted diffuse flux in this simple model,

$$E_\nu^2 \Phi_\nu \sim 10^{-9}\ \mathrm{GeV\,cm^{-2}\,s^{-1}\,sr^{-1}}\,, \qquad (22)$$

is just the expectation given in Eq.(7), which was based on the assumption of complete trapping of charged particles (recall that $\kappa = 0.25$ and, for single $p\gamma$ collisions, $\epsilon_\pi \sim 0.2$). Of course a more sophisticated estimate can be made using our results in Fig.10 when we know more about the relative contributions from the different possible sources to the overall cosmic ray flux, as well as the relative (possibly energy dependent) weighting of heavy nuclei with respect to protons. Being conservative, presently we can only argue that the overall cosmic neutrino flux should be reduced by about 75%.

In closing, we stress that the diffuse neutrino flux has an additional component originating in the energy losses of ultra-high energy cosmic rays *en route* to Earth. The main energy loss process here is photo-pion production in the CMB, which causes the steepening of the cosmic ray spectrum beyond $10^{19.7}$ eV. The decay of charged pions produced in this process results in a diffuse flux of "cosmogenic" neutrinos [78], which is comparable to the fluxes shown in Fig. 10. If there are heavy nuclei in ultra-high energy cosmic rays then they will preferentially lose energy through photo-disintegration rather than photo-pion production, so the cosmogenic neutrino flux will also be suppressed as has been discussed elsewhere [79].

Equipped with the fluxes shown in Figs. 10 and 11, we now proceed to determine the expected event rates in a next generation neutrino telscope such as IceCube. We do not consider the cosmogenic flux so these rates are conservative.

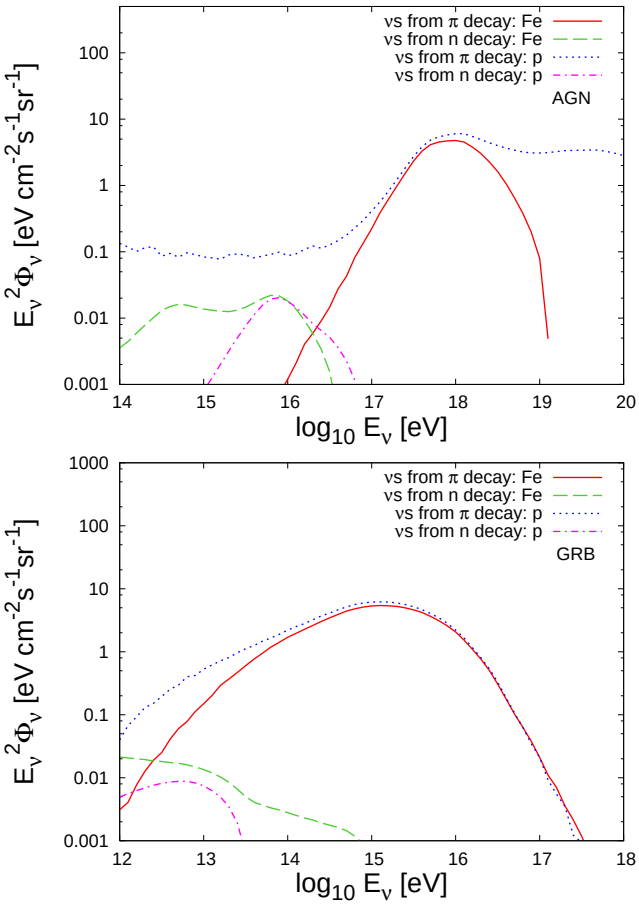

FIG. 10: The neutrino spectra produced by protons and iron nuclei being accelerated in AGN (top) and GRBs (bottom). The fluxes have been normalized following the Waxman-Bahcall prescription, namely assuming that all ultra-high energy particles observed on Earth are protons.

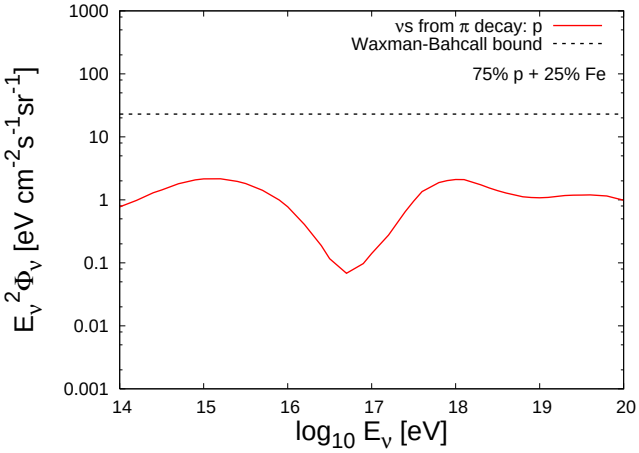

FIG. 11: The neutrino spectrum produced by protons undergoing acceleration in AGN and GRBs which are assumed to contribute equally to the cosmic ray protons observed at Earth. The Waxman-Bahcall bound, as obtained from Eq. (3) by setting $\epsilon_\pi = \xi_Z = 1$, is also shown for comparison.

V. EXPECTED EVENT RATES AT ICECUBE

The IceCube neutrino telescope is currently under construction at the South Pole. When complete, it will comprise a cubic-kilometer of ultra-clear ice about 2 km below the surface, instrumented with long strings of sensitive photon detectors [80]. We focus on this experiment as it is the most advanced of its kind, however the event rates estimated below will also apply to e.g. the KM3 undersea experiment being planned for the Mediterranean.

IceCube is designed to observe muon tracks and showers produced by neutrino charged current (CC) and neu-

tral current (NC) interactions in and around the instrumented volume. The probability of detecting a neutrino passing through the detector from its muon track is given by

$$P_{\nu\to\mu}(E_\nu,\theta_{\rm zenith}) = \sigma_{\nu N}^{\rm CC}(E_\nu)\, n\, R_\mu(E_\mu,\theta_{\rm zenith}), \quad (23)$$

where $\sigma_{\nu N}^{\rm CC}(E_\nu)$ is the charged current neutrino-nucleon cross section [81], n is the number density of nucleons in the ice, and the muon range $R_\mu(E_\mu,\theta_{\rm zenith})$ is the average distance traveled by a muon of energy E_μ before it is degraded below some threshold energy (taken to be 100 GeV). This quantity depends on the zenith angle of the incoming neutrino as only quasi-horizontal or upgoing events can benefit from longer muon ranges. At the energies we are most concerned with, the majority of muon events will be quasi-horizontal.

The expected muon event rate is

$$\frac{d\mathcal{N}_\mu}{dt} = \int dE_\nu\, d\Omega\, \Phi_{\nu_\mu}(E_\nu)\, P_{\nu\to\mu}(E_\nu,\theta_{\rm zenith})\, A_{\rm eff}\,, \quad (24)$$

where $\Phi_{\nu_\mu}(E_\nu) = \Phi_\nu(E_\nu)/3$ is the flux of muon neutrinos and $A_{\rm eff} \approx 1$ km^2 is the effective area of the detector [80]. Similarly, the expected number of shower events is

$$\frac{d\mathcal{N}_{\rm S}}{dt} = \sum_\alpha \int dE_\nu\, d\Omega\, \Phi_{\nu_\alpha}(E_\nu)\, \sigma_{\nu N}^{\rm CC(NC)}(E_\nu)\, V_{\rm eff}\,, \quad (25)$$

where $\sigma_{\nu N}^{\rm CC(NC)}$ is the CC (NC) neutrino-nucleon cross section and $V_{\rm eff}$ is the effective volume for detection of showers [82]. The sum is over ν_e and ν_τ CC interactions and all NC interactions, and we assume $\Phi_{\nu_\alpha}(E_\nu) = \Phi_\nu(E_\nu)/3$ where $\alpha = e,\mu,\tau$. Electron neutrino, CC induced showers carry all of the incoming neutrino energy, whereas muon neutrino (CC or NC) induced showers carry away an energy of $(1-y)\,E_\nu$. Tau neutrino NC showers have an energy $(1-y)\,E_\nu$, whereas tau neutrinos CC events with energies below $E_\nu \sim$ PeV generate showers with the full energy of the incoming neutrino. We assume that only showers with energies greater than 3 TeV can be identified at IceCube.

In Table 1, we show the predicted event rates for the various cosmic ray accelerators considered earlier. We also show the effect on the rates if the threshold for both muons and showers is taken to be 100 TeV — a cut at this higher energy is adequate to eliminate essentially all background from muon bremsstrahlung radiation near the detector and from muons produced in cosmic ray showers in the atmosphere. Moreover, the steeply falling flux of atmospheric neutrinos is negligible above this energy, so this cut generates a very pure sample of extraterrestrial neutrinos. The labels "protons" and "iron" denote the species of particle which are accelerated by the source (rather than what actually escapes).

As expected, the event rates from GRBs are similar regardless of whether protons or iron nuclei are accelerated, as the latter are almost entirely disintegrated by the surrounding radiation fields. Values for starburst galaxies are not given in the table as the rates (from $p\gamma$ interactions) are well below the sensitivity of IceCube and other next generation neutrino telescopes.

TABLE I: Predicted event rates at IceCube for various sources of high energy neutrinos, with the muon energy threshold set to 0.1 (100) TeV and the threshold for showers set to be 3 (100) TeV. The labels "protons" and "iron" denote the type of particle assumed to be accelerated, rather than what actually escapes (iron nuclei do not escape intact from GRBs, in particular). The label "UHECR Best Fit" denotes the case where 75% of the ultra high energy cosmic rays arriving at Earth are protons (assumed to be accelerated equally by GRB and AGN) and 25% are iron nuclei (assumed to be accelerated by starburst galaxies).

Source	$d\mathcal{N}_\mu/dt$	$d\mathcal{N}_{\rm S}/dt$
AGN (protons)	1.2 (0.34) yr^{-1}	0.45 (0.089) yr^{-1}
AGN (iron)	0.23 (0.13) yr^{-1}	0.045 (0.037) yr^{-1}
GRB (protons)	16. (3.4) yr^{-1}	6.3 (2.2) yr^{-1}
GRB (iron)	12. (2.8) yr^{-1}	4.5 (1.9) yr^{-1}
UHECR Best Fit	6.5 (1.4) yr^{-1}	2.5 (0.86) yr^{-1}

VI. CONCLUSIONS

We have studied the role that heavy nuclei play in the generation of neutrinos in possible astrophysical sources of high energy cosmic rays. During acceleration the nuclei may be completely photo-disintegrated into their constituent nucleons and we find this indeed happens in GRBs, resulting in the outgoing cosmic rays being proton dominated. The neutrino flux is then left largely unchanged from previous estimates which had ignored the possibility of nuclei being accelerated as well as protons. At the other extreme, sources such as starburst galaxies hardly disintegrate accelerated nuclei, enabling such particles to escape and to contribute to the observed ultra-high energy cosmic ray spectrum, largely without contributing to the cosmic neutrino flux. In AGN the situation is in between, with nuclei being fully disintegrated only at the highest energies, so the neutrino flux is suppressed at lower energies.

The likely possibility of a substantial fraction of nuclei in ultra-high energy cosmic rays implies therefore a somewhat reduced expectation for the neutrino flux from their cosmic sources. In particular, as the spectrum and elongation length in the atmosphere of ultra-high energy cosmic rays appears to be best fitted by a mixture of 25% iron nuclei and 75% protons, the overall neutrino flux is reduced somewhat relative to the expectation for an all-proton cosmic ray spectrum.

As next generation neutrino telescopes such as IceCube begin operation, it becomes increasingly important to refine the expectations for detection of high energy neu-

trinos from the sources of cosmic rays. We have taken into account recent data on ultra-high energy cosmic rays to provide updated estimates of the neutrino fluxes to be expected from various types of possible extragalactic sources. The actual detection of cosmic neutrinos will in turn thus provide crucial information on the nature of the long sought sources of cosmic rays.

Acknowledgments

DH is supported by the US DoE and by NASA grant NAG5-10842. SS acknowledges a PPARC Senior Fellowship award (PPA/C506205/1). We thank Johannes Knapp for providing the simulated values of $X_{\max}$.

[1] For a review, see: F. Halzen and D. Hooper, Rept. Prog. Phys. **65**, 1025 (2002).
[2] A. Achterberg *et al.* [IceCube Collaboration], Phys. Rev. Lett. **97**, 221101 (2006); Astropart. Phys. **26**, 282 (2006); arXiv:astro-ph/0611063; arXiv:astro-ph/0702265.
[3] V. Niess [ANTARES Collaboration], AIP Conf. Proc. **867**, 217 (2006).
[4] I. Kravchenko *et al.*, Phys. Rev. D **73**, 082002 (2006).
[5] S. W. Barwick *et al.* [ANITA Collaboration], Phys. Rev. Lett. **96**, 171101 (2006).
[6] V. Van Elewyck [Pierre Auger Collaboration], AIP Conf. Proc. **809**, 187 (2006).
[7] For a survey of possible sources and event rates in km^3 detectors see e.g., W. Bednarek, G. F. Burgio and T. Montaruli, New Astron. Rev. **49**, 1 (2005); M. D. Kistler and J. F. Beacom, Phys. Rev. D **74**, 063007 (2006); A. Kappes, J. Hinton, C. Stegmann and F. A. Aharonian, arXiv:astro-ph/0607286.
[8] A. Levinson and E. Waxman, Phys. Rev. Lett. **87**, 171101 (2001); C. Distefano, D. Guetta, E. Waxman and A. Levinson, Astrophys. J. **575**, 378 (2002); F. A. Aharonian, L. A. Anchordoqui, D. Khangulyan and T. Montaruli, J. Phys. Conf. Ser. **39**, 408 (2006).
[9] J. Alvarez-Muniz and F. Halzen, Astrophys. J. **576**, L33 (2002); F. Vissani, Astropart. Phys. **26**, 310 (2006).
[10] F. W. Stecker, C. Done, M. H. Salamon and P. Sommers, Phys. Rev. Lett. **66**, 2697 (1991) [Erratum-ibid. **69**, 2738 (1992)]; F. W. Stecker, Phys. Rev. D **72**, 107301 (2005); A. Atoyan and C. D. Dermer, Phys. Rev. Lett. **87**, 221102 (2001); L. A. Anchordoqui, H. Goldberg, F. Halzen and T. J. Weiler, Phys. Lett. B **600**, 202 (2004).
[11] E. Waxman and J. N. Bahcall, Phys. Rev. Lett. **78**, 2292 (1997); C. D. Dermer and A. Atoyan, Phys. Rev. Lett. **91**, 071102 (2003); D. Guetta, D. Hooper, J. Alvarez-Muniz, F. Halzen and E. Reuveni, Astropart. Phys. **20**, 429 (2004); J. Alvarez-Muniz, F. Halzen and D. W. Hooper, Phys. Rev. D **62**, 093015 (2000).
[12] A. Loeb and E. Waxman, JCAP **0605**, 003 (2006).
[13] S. Inoue, G. Sigl, F. Miniati and E. Armengaud, arXiv:astro-ph/0701167.
[14] E. Waxman and J. N. Bahcall, Phys. Rev. D **59**, 023002 (1999); Phys. Rev. D **64**, 023002 (2001).
[15] K. Mannheim, R. J. Protheroe and J. P. Rachen, Phys. Rev. D **63**, 023003 (2001); arXiv:astro-ph/9908031.
[16] M. Ahlers, L. A. Anchordoqui, H. Goldberg, F. Halzen, A. Ringwald and T. J. Weiler, Phys. Rev. D **72**, 023001 (2005).
[17] E. Waxman, Astrophys. J. **452**, L1 (1995).
[18] Note that the neutrino spectral shape can deviate from that for protons if the Feynman plateau is not flat in pseudo-rapidity space: L. Anchordoqui, H. Goldberg and C. Nunez, Phys. Rev. D **71**, 065014 (2005). This is in fact suggested by Tevatron data; F. Abe *et al.* [CDF Collaboration], Phys. Rev. D **41**, 2330 (1990).
[19] J. G. Learned and S. Pakvasa, Astropart. Phys. **3**, 267 (1995); F. Halzen and D. Saltzberg, Phys. Rev. Lett. **81**, 4305 (1998); J. F. Beacom, N. F. Bell, D. Hooper, S. Pakvasa and T. J. Weiler, Phys. Rev. D **68**, 093005 (2003) [Erratum-ibid. D **72**, 019901 (2005)].
[20] L. A. Anchordoqui, H. Goldberg, F. Halzen and T. J. Weiler, Phys. Lett. B **593**, 42 (2004); L. A. Anchordoqui, H. Goldberg, F. Halzen and T. J. Weiler, Phys. Lett. B **621**, 18 (2005).
[21] A. M. Hillas, Ann. Rev. Astron. Astrophys. **22**, 425 (1984).
[22] For a general discussion on the acceleration time-scale in these sources, see e.g., D. F. Torres and L. A. Anchordoqui, Rept. Prog. Phys. **67**, 1663 (2004).
[23] M. C. Begelman, B. Rudak and M. Sikora, Astrophys. J. **362**, 38 (1990).
[24] M. J. Chodorowski, A. A. Zdziarski, and M. Sikora, Astrophys. J. **400**, 181 (1992).
[25] S. Michalowski, D. Andrews, J. Eickmeyer, T. Gentile, N. Mistry, R. Talman and K. Ueno, Phys. Rev. Lett. **39**, 737 (1977).
[26] J. L. Puget, F. W. Stecker and J. H. Bredekamp, Astrophys. J. **205**, 638 (1976).
[27] D. Hooper, S. Sarkar and A. M. Taylor, Astropart. Phys. **27**, 199 (2007).
[28] The non-thermal energy release in GRBs is much smaller than that output by AGN.
[29] P. L. Biermann and P. A. Strittmatter, Astrophys. J. **322**, 643 (1987); R. J. Protheroe and A. P. Szabo, Phys. Rev. Lett. **69**, 2885 (1992); J. P. Rachen and P. L. Biermann, Astron. Astrophys. **272**, 161 (1993); J. P. Rachen, T. Stanev and P. L. Biermann, Astron. Astrophys. **273**, 377 (1993).
[30] R. C. Hartman *et al.* [EGRET Collaboration], Astrophys. J. Suppl. **123**, 79 (1999).
[31] M. Punch *et al.*, Nature **358**, 477 (1992); D. Petry *et al.* [HEGRA Collaboration], Astron. Astrophys. **311**, L13 (1996); P. M. Chadwick *et al,* Astrophys. J. **513**, 161 (1999).
[32] C. D. Dermer, R. Schlickeiser, and A. Mastichiadis, Astron. Astrophys. **256**, L27 (1992); S. D. Bloom and A. P. Marscher, Astrophys. J. **461**, 657 (1996).
[33] A. Dar and A. Laor, Astrophys. J. **478**, L5 (1997).
[34] M. Boettcher, Astrophys. J. **515**, L21 (1999).
[35] C. D. Dermer and R. Schlickeiser, Astrophys. J. **416**, 458 (1993).
[36] F. W. Stecker, Phys. Rev. Lett. **21**, 1016 (1968).
[37] G. J. Fishman and C. A. Meegan, Ann. Rev. Astron. Astrophys. **33**, 415 (1995).
[38] For a list of papers related to SWIFT, see:

http://swift.gsfc.nasa.gov/docs/swift/results/publist/
[39] B. Link and R. I. Epstein, Astrophys. J. **466**, 764 (1996).
[40] C. A. Meegan *et al.*, Nature **355**, 143 (1992).
[41] M. R. Metzger *et al.*, Nature **387**, 878 (1997).
[42] See e.g., T. Piran, Phys. Rept. **314** (1999) 575; Phys. Rept. **333** (2000) 529.
[43] For a recent review of GRB phenomenology, see: P. Meszaros, Rept. Prog. Phys. **69**, 2259 (2006).
[44] E. Waxman, Lect. Notes Phys. **576**, 122 (2001).
[45] M. Milgrom and V. Usov, Astrophys. J. **449**, L37 (1995); E. Waxman, Phys. Rev. Lett. **75**, 386 (1995); M. Vietri, Phys. Rev. Lett. **78**, 4328 (1997); S. D. Wick, C. D. Dermer and A. Atoyan, Astropart. Phys. **21**, 125 (2004).
[46] D. Band *et al.* Astrophys. J. **413**, 281 (1993).
[47] F. Halzen, Proc. TASI 98, Boulder, ed. K. Oliver, p.524 (1998).
[48] J. W. Elbert and P. Sommers, Astrophys. J. **441**, 151 (1995); L. A. Anchordoqui, G. E. Romero and J. A. Combi, Phys. Rev. D **60**, 103001 (1999).
[49] L. A. Anchordoqui, J. F. Beacom, H. Goldberg, S. Palomares-Ruiz and T. J. Weiler, arXiv:astro-ph/0611580; arXiv:astro-ph/0611581.
[50] The factor $9/(4R^2)$ results from calculating $\int d^3\vec{r}_1 \quad \int d^3\vec{r}_2 \quad |\vec{r}_1 - \vec{r}_2|^{-2} \quad (4\pi R^3/3)^{-2}$, where $\vec{r}_1$ is the position of a star and $\vec{r}_2$ is the position of an observer (the position of the reaction), in a region of radius R uniformly filled with sources.
[51] D. A. Forbes, M. J. Ward, V. Rotaciuc, M. Blietz, R. Genzel, S. Drapatz, P. P van der Werf and A. Krabbe, Astrophys. J. **406**, L11 (1993).
[52] P. Chanial, H. Flores, B. Guiderdoni, D. Elbaz, F. Hammer and L. Vigroux, arXiv:astro-ph/0610900.
[53] P. O. Lagage and C. J. Cesarsky Astron. Astrophys. **118**, 223 (1983).
[54] S. P. Lai, J. M. Girart and R. Crutcher, Astrophys. J. **598**, 392 (2003).
[55] W. Bednarek, Mon. Not. Roy. Astron. Soc. **345**, 847 (2003); W. Bednarek and R. J. Protheroe, Astropart. Phys. **16**, 397 (2002).
[56] P. Blasi and A. V. Olinto, Phys. Rev. D **59**, 023001 (1999).
[57] F. W. Stecker, Astropart. Phys. **26**, 398 (2007); F. W. Stecker, arXiv:astro-ph/0610208.
[58] A γ-ray signal from the nearby starburst galaxy NGC253 was reported by the CANGAROO-II Collaboration, but their subsequent re-analysis of the data is consistent with the expectation from backgrounds: C. Itoh *et al.* [CANGAROO-II Collaboration], Astron. Astrophys. **396**, L1 (2002) [Erratum-ibid. **462**, 67 (2007)].
[59] T. A. Thompson, E. Quataert, E. Waxman and A. Loeb, arXiv:astro-ph/0608699.
[60] D. J. Bird *et al.* [Fly's Eye Collaboration], Phys. Rev. Lett. **71** 3401 (1993).
[61] D. R. Bergman [HiRes Collaboration], Nucl. Phys. Proc. Suppl. **136**, 40 (2004).
[62] T. Abu-Zayyad *et al.*, [HiRes-MIA Collaboration], Astrophys. J. **557**, 686 (2001).
[63] M. Nagano *et al.*, J. Phys. G **18**, 423 (1992).
[64] V. Berezinsky, A. Z. Gazizov and S. I. Grigorieva, Phys. Rev. D **74**, 043005 (2006); R. U. Abbasi *et al.* [HiRes Collaboration], Phys. Rev. Lett. **92**, 151101 (2004).
[65] V. Berezinsky, A. Z. Gazizov and S. I. Grigorieva, Phys. Lett. B **612**, 147 (2005).
[66] V. S. Berezinsky, S. I. Grigorieva and B. I. Hnatyk, Astropart. Phys. **21**, 617 (2004).
[67] See Fig. 21 in L. Anchordoqui, M. T. Dova, A. Mariazzi, T. McCauley, T. Paul, S. Reucroft and J. Swain, Annals Phys. **314**, 145 (2004).
[68] D. Allard, E. Parizot, E. Khan, S. Goriely and A. V. Olinto, Astron. Astrophys. **443**, L29 (2005); D. Allard, E. Parizot and A. V. Olinto, Astropart. Phys. **27** 61 (2007).
[69] T. Abu-Zayyad *et al.* [High Resolution Fly's Eye Collaboration], Astropart. Phys. **23**, 157 (2005).
[70] P. Sommers *et al.* [Pierre Auger Collaboration], arXiv:astro-ph/0507150.
[71] R. U. Abbasi *et al.* [HiRes Collaboration], Astrophys. J. **622**, 910 (2005).
[72] B. N. Afanasiev *et al.* [Yakutsk Collaboration], Proc. Tokyo Workshop on Techniques for the Study of the Extremely High Energy Cosmic Rays, ed. M. Nagano (1993).
[73] J. Knapp, private communication.
[74] J. Ranft, Phys. Rev. D **51**, 64 (1995).
[75] R. S. Fletcher, T. K. Gaisser, P. Lipari and T. Stanev, Phys. Rev. D **50**, 5710 (1994); J. Engel, T. K. Gaisser, T. Stanev and P. Lipari, Phys. Rev. D **46**, 5013 (1992).
[76] N. N. Kalmykov, S. S. Ostapchenko and A. I. Pavlov, Nucl. Phys. Proc. Suppl. **52B**, 17 (1997).
[77] It is important to stress that the Auger data are still at a preliminary stage and the reconstruction procedures are still to be finalised. However, even allowing for the systematic uncertainties still present, it does appear that at the highest energies fewer events are seen than expected from the AGASA analysis.
[78] V. S. Berezinsky and G. T. Zatsepin, Phys. Lett. B **28**, 423 (1969); F. W. Stecker, Astrophys. J. **228**, 919 (1979); R. Engel, D. Seckel and T. Stanev, Phys. Rev. D **64**, 093010 (2001); Z. Fodor, S. D. Katz, A. Ringwald and H. Tu, JCAP **0311**, 015 (2003); D. De Marco, T. Stanev and F. W. Stecker, Phys. Rev. D **73**, 043003 (2006).
[79] D. Hooper, A. Taylor and S. Sarkar, Astropart. Phys. **23**, 11 (2005); M. Ave, N. Busca, A. V. Olinto, A. A. Watson and T. Yamamoto, Astropart. Phys. **23**, 19 (2005)
[80] J. Ahrens *et al.* [IceCube Collaboration], Astropart. Phys. **20**, 507 (2004).
[81] R. Gandhi, C. Quigg, M. H. Reno and I. Sarcevic, Phys. Rev. D **58**, 093009 (1998); L. A. Anchordoqui, A. M. Cooper-Sarkar, D. Hooper and S. Sarkar, Phys. Rev. D **74**, 043008 (2006).
[82] See Fig. 3 in L. Anchordoqui and F. Halzen, Annals Phys. **321**, 2660 (2006).